

# Variations in the Total Electron Content during the Powerful Typhoon of August 5–11, 2006, near the Southeastern Coast of China

E. L. Afraimovich<sup>a</sup>, S. V. Voeykov<sup>a</sup>, A. B. Ishin<sup>a</sup>, N. P. Perevalova<sup>a</sup>, and Yu. Ya. Ruzhin<sup>b</sup>

<sup>a</sup> *Institute of Solar–Terrestrial Physics, Siberian Branch, Russian Academy of Sciences (ISZF SO RAN),  
P.O. Box 4026, Irkutsk, 664033 Russia*

<sup>b</sup> *Institute of Terrestrial Magnetism, Ionosphere, and Radiowave Propagation, Russian Academy of Sciences,  
Troitsk, Moscow oblast, 142190 Russia  
e-mail: afra@iszf.irk.ru*

Received February 7, 2008

**Abstract**—The variations in the total electron content (TEC), obtained from the data of 11 ground-based GPS stations in the region (5°S – 80°N; 110 – 160°E) in the period August 2–15, 2006, have been analyzed in order to search for possible ionospheric manifestations of the SAOMAI powerful typhoon (August 5–11, 2006) near the south–eastern coast of China. The global TEC maps (GIM) have also been used. In the region of the typhoon action during the magnetic storm of August 7, 2006, an intensification of the TEC variations in the evening local time within the 32–128 min periods range was detected. However, this effect was most probably caused by the dynamics of the irregular structure of the equatorial anomaly and by the disturbed geomagnetic situation ( $Kp \sim 3–6$ ,  $Dst$  varied from  $-74$  to  $-153$  nT). The analysis of the diurnal variations in the absolute values of TEC and TEC variations with periods of 2–25 min did not reveal a substantial increase in the intensity and changes in the spectrum of the TEC variations in the period of typhoon action as compared to the adjacent days. Thus, we failed to detect ionospheric disturbances unambiguously related to the SAOMAI typhoon.

PACS numbers: 94.20.Ji, 92.60.Ax

DOI: 10.1134/S0016793208050113

## 1. INTRODUCTION

Solar and geomagnetic activities play a dominant role in the formation, structure, and dynamic regime of the ionosphere. However, some features in the variations in ionospheric parameters cannot be explained assuming that the ionosphere is isolated from the underlying atmospheric layers. Therefore, a tendency to consider the atmosphere of the Earth as a united dynamical system has been finally accepted in geophysics, and studying the atmosphere–ionosphere coupling became one of promising branches of geophysics. It is usually considered that this coupling is mainly caused by upward propagation of planetary (with periods of a few days), tidal (several hours), and acoustic gravity (10–150 min) waves.

The search for meteorological effects in the ionosphere, as a rule, includes a detection of correlation between the variations in the ionospheric and tropospheric parameters. The majority of works in this field are devoted to studying long-scale (with periods varying from a few hours to 30 days) disturbances in the ionosphere related to planetary and tidal waves [Forbes et al., 2000; Kazimirovsky and Kokourov, 1979; Pancheva et al., 2002].

At the same time, the publications dedicated to troposphere–ionosphere coupling and internal atmospheric waves repeatedly assumed that powerful meteorological disturbances (cyclones, hurricanes, typhoons, tornado, thunderstorms, etc.) should cause electric fields and acoustic gravity waves (AGWs). Under favorable conditions, AGWs can penetrate up to ionospheric heights and can be observed there as traveling ionospheric disturbances (TIDs) [Cowling et al., 1971; Hocke and Shlegel, 1996; Kazimirovsky and Kokourov, 1979; Sorokin et al., 2001; Waldock and Jones, 1984].

Until recently, TIDs related to meteorological disturbances have been detected mainly based on the measurements of the Doppler frequency shift or Faraday rotation of the sounding signal polarization plane. The series of works [Davies and Jones, 1971, 1973; Prasad et al., 1975] describe quasi-sinusoidal oscillations registered during strong thunderstorms. Bertin et al. [1975] calculated the azimuth and horizontal velocity of a few wave-like TIDs with periods of 20–100 min, presumably related to meteorological processes. It turned out that the zones, where registered TIDs are probably generated, are located in the troposphere and coincide with the regions of decreased

atmospheric pressure in the cyclone formation regions. Using the grate of Doppler installations in northern Taiwan, Huang et al. [1985] studied TID parameters during 12 typhoons in 1982–1983. Huang et al. [1985] managed to detect an ionospheric response in the form of quasiperiodic variations with a characteristic period of 13–14 min only for two events. The measured periods were close to the periods obtained from the microbarograph data.

However, the existence of meteorological TIDs has not yet been reliably confirmed experimentally because it is difficult to detect weak ionospheric disturbances, separate such TIDs from the general background of ionospheric oscillations, and to identify a TID source. In addition, meteorological disturbances are weakly localized in time (they exist up to a few days), and they are generated in the region probably extending over more than 1000 km.

During the recent decade, technologies of remote diagnostics of the ionosphere using signals from the GPS satellite radio navigation system have been rapidly developed. At ISZF SO RAN, the scientific principles were developed, and a unique bundled software GLOBDET for global monitoring of ionospheric disturbances was elaborated based on measurements of TEC variations using spaced GPS receivers [Afraimovich, 2000]. New capacities of the GLOBDET detector will probably make it possible to overcome the difficulties in detecting ionospheric disturbances of a meteorological origin.

The goal of this paper is to search for possible ionospheric manifestations of the SAOMAI powerful typhoon (August 7–11, 2006) near the southeastern coast of China. For this purpose, we used the data on TEC variations obtained at the ground-based GPS stations in the Asian–Pacific region (0–80°N; 60–220°E) on August 2–17, 2006, and the global TEC maps (GIM [Mannucci et al., 1998]).

## 2. GENERAL INFORMATION ON THE EXPERIMENT AND DATA PROCESSING METHOD

The dashed curve in Fig. 1a shows the trajectory of the SAOMAI typhoon center on August 5–11, 2006. Asterisks show the typhoon positions at 0000 UT on each day. The corresponding dates are shown nearby. The data concerning the typhoon were taken from the site (<http://www.solar.ifa.hawaii.edu/Tropical/>). Filled circles correspond to the GPS stations the data of which were available in the Internet (<http://sopac.ucsd.edu>). Table shows the names and coordinates of these stations. Figure 1a indicates that the typhoon was mostly over open ocean, where the density of the GPS stations is very low, and it was registered at the China territory only on the last day of its existence. Such position of the typhoon substantially

Coordinates of used stations

Station	Latitude	Longitude
DAEJ	36.3994288	127.3744786
GUAM	13.5893293	144.8683612
KGNI	35.7106552	139.4881208
KSMV	35.9556837	140.6576748
MIZU	39.1350662	141.1336594
PIMO	14.6357194	121.0777323
SHAO	31.0996427	121.2004436
SUWN	37.2755147	127.0542402
TSKB	36.1056798	140.0874965
USUD	36.1331106	138.3620437
TCMS	24.7982360	120.9873891

complicated registration of possible ionospheric responses according to the GPS data.

The geomagnetic situation can be characterized as disturbed. The time variations in the *Kp* geomagnetic disturbance index (black curve) and *Dst* (gray curve) are shown in Fig. 2d. A magnetic storm with SSC at 0036 UT was registered on August 7, 2006. During the storm, the *Kp* index values reached 5–6, and the *Dst* values varied from –74 to –153 nT.

The GPS technology makes it possible to detect wave disturbances in the ionosphere based on phase variations in oblique TEC  $I_s$  [Hofmann-Wellenhof et al., 1992]:

$$I_s = \frac{1}{40.308} \frac{f_1^2 f_2^2}{(f_1^2 - f_2^2)} [(L_1 \lambda_1 - L_2 \lambda_2) + \text{const} + nL], \quad (1)$$

where  $L_1 \lambda_1$  and  $L_2 \lambda_2$  are increments of the radiosignal phase path caused by the phase delay in the ionosphere (m),  $L_1$  and  $L_2$  are the number of complete phase rotations,  $\lambda_1$  and  $\lambda_2$  are the wavelengths (m) for  $f_1$  and  $f_2$  frequencies (Hz), const is some unknown initial phase path (m), and  $nL$  is the error in determining the phase path (m).

Phase measurements in the GPS system are conducted with high accuracy, when the error of TEC determination at 30-s averaging intervals does not exceed  $10^{14} \text{ m}^{-2}$ , although the initial TEC value remains unknown [Hofmann-Wellenhof et al., 1992]. This makes it possible to detect ionization irregularities and wave processes in the ionosphere within a wide range of amplitudes (up to  $10^{-4}$  of the diurnal variation in TEC) and periods (from days to 5 min). Below we will use the unit of TEC (TECU), equal to  $10^{16} \text{ m}^{-2}$ , commonly accepted in the literature.

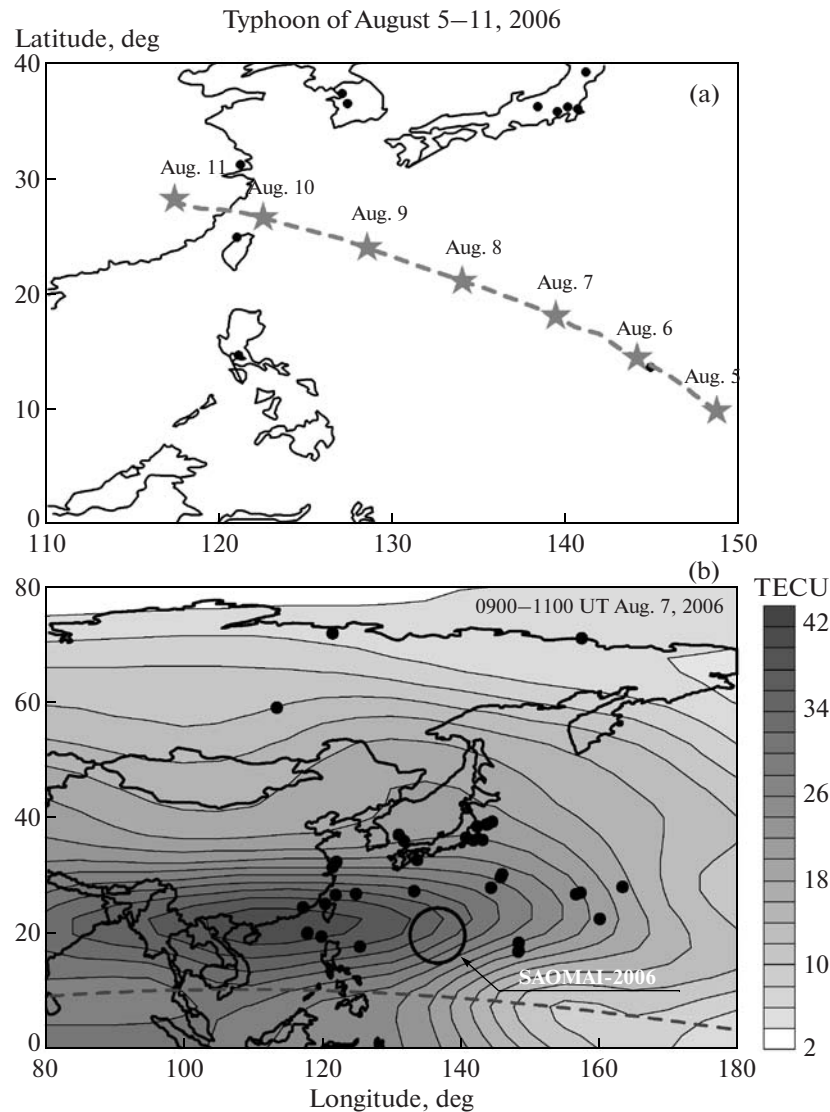


**Fig. 1.** (a) General geometry of the experiment. Filled circles show the GPS stations. Asterisks show the everyday position of the typhoon center at 0000 UT. (b) Gray dashed curve shows the geomagnetic equator. Gradations of gray demonstrate the TEC map (GIM) for 0900–1100 UT on August 7, 2006. Filled circles mark the position of subionospheric points corresponding to the TEC variation maximums at 0900–1100 UT on August 7, 2006. The position of the typhoon at 1000 UT on August 7, 2006, is shown by the circle.

TEC disturbance amplitudes are normalized by transforming the “oblique” TEC  $I_s$  into the equivalent “vertical” value  $I$  [Klobuchar, 1986]:

$$I = I_s \cos \left[ \arcsin \left( \frac{R_E}{R_E + h_{\max}} \cos \theta_s \right) \right] \quad (2)$$

where  $R_E$  is the Earth’s radius, and  $h_{\max}$  is the height of the ionospheric  $F_2$  layer maximum;  $S$  is the angle of sight to the satellite.

The most reliable determinations of the ionospheric disturbance parameters correspond to high elevation angles  $\theta_s$  of the ray to the satellite because the effects of sphericity become fairly small in this case. In

our case all results were obtained for the elevation angles  $\theta_s$  more than  $30^\circ$ .

From the entire set of TEC data we chose continuous series  $I(t)$  with a duration of 2.3 h. Thus, for each day we obtained the TEC data for 22 overlapping periods at an interval of 1 h. The TEC series  $I(t)$  were filtered by the running mean method within three ranges of periods: 2–10, 10–25, and 32–128 min (the  $dI(t)$  series). For each  $dI(t)$  series, the standard deviations  $\sigma$  were calculated. Then, for each 2.3-h interval, the  $\sigma$  values were averaged over all  $dI(t)$  series filtered within the given range of periods  $S = [\sum \sigma_i] / m$ , where  $i = 1, 2, \dots, m$ ,  $m$  being the number of  $dI(t)$  series. In such a way we obtained the  $S_L(t)$ ,  $S_M(t)$ , and  $S_S(t)$  series of TEC

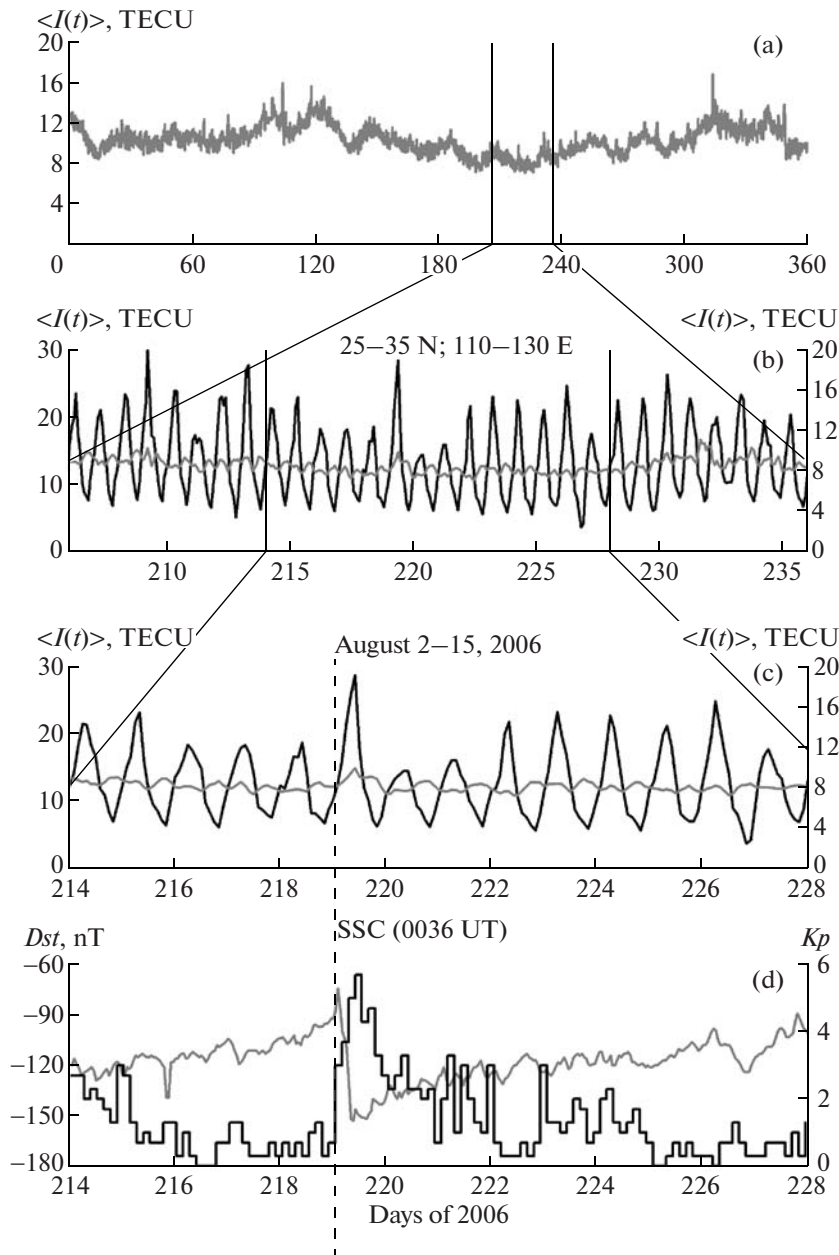


**Fig. 2.** (a) Variations in TEC averaged over the globe for 2006. The time variations in the TEC values averaged over the globe (gray curve) and over the (25°–35°N; 110°–130°E) region (black curve) for the following days in the year: (b) 206–236 and (c) 214–228. (d) Variations in the values of the  $Kp$  (black curve) and  $Dst$  (gray curve) indices.

intensity variations within three range of periods corresponding to large-scale (32–128 min), medium-scale (10–25 min), and small-scale (2–10 min) disturbances, respectively.

We also used the data of the GIM maps [Mannucci et al., 1998] to determine the absolute vertical TEC values averaged over the entire globe and over the region where SAOMAI activity was the highest (25°–35°N; 110°–130°E).

### 3. TEC VARIATIONS IN THE SAOMAI TYPHOON REGION

We analyzed the TEC variations obtained from the GIM data, averaged over the globe and the region of maximum typhoon activity (Fig. 2). Figure 2a shows the changes in the absolute TEC values, averaged over the globe for 2006. Figure 2 also presents the time variations in the TEC values, averaged over the globe (gray curve) and the region (25°–35°N; 110°–130°E)

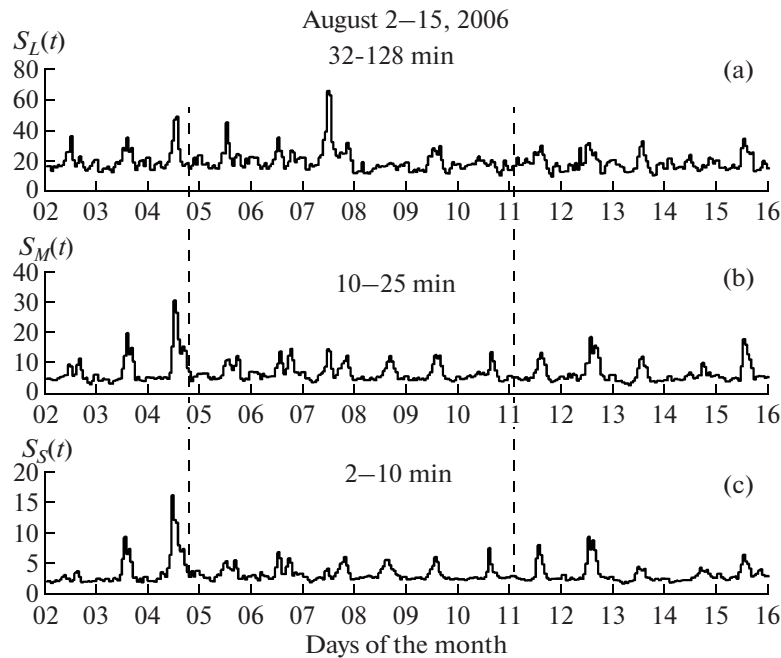


**Fig. 3.** (a)–(c) Intensities of the  $S_L(t)$ ,  $S_M(t)$ , and  $S_S(t)$  series of TEC variations for the region of typhoon action ( $5^{\circ}\text{S}$ – $40^{\circ}\text{N}$ ;  $110^{\circ}$ – $160^{\circ}\text{E}$ ) filtered within the ranges of periods 32–128, 10–25, and 2–10 min, respectively. The graphs were drawn for the period August 2–15, 2006.

(black curve), for days (b) 206–236 and (c) 214–228 in the year.

The response to the magnetic storm of August 7, 2006, is traced in the changes in TEC averaged over the globe (Figs. 2b, 2c, gray curve). It is clear that TEC increases over the entire globe after sudden commencement. The same picture can also be observed for regional TEC (Figs. 2b, 2c, black curve). A decrease in the maximum TEC values on the days after the storm with a gradual recovery of the undisturbed level is clearly defined in the time variations in regional TEC. Such a behavior of the electron density and TEC is quite typical of geomagnetic storms and was described in numerous publications (see, e.g., [Buonsanto, 1999]).

If we compare regional TEC during the existence of the typhoon with the preceding and following days, we cannot come to the conclusion that TEC increases during typhoon existence. In addition to the response to the magnetic storm, other TEC variation maximums, comparable with this response, were registered during the considered period.

The series of TEC variation intensities were also analyzed within three ranges of periods (Fig. 3). Figure 3 shows the  $S_L(t)$ ,  $S_M(t)$ , and  $S_S(t)$  series of TEC variation intensity for three ranges of periods. Vertical dashed lines show the period when the SAOMAI typhoon was observed.

Figure 3a indicates that, during the action of the typhoon, the intensity of  $S_L(t)$  variations in TEC with

periods of 32–128 min increased only during the magnetic storm of August 7, 2006 (Fig. 2d). On the remaining days of the typhoon existence, the  $S_L(t)$  series has no substantial differences as compared to the adjacent days. To determine the spatial localization of large-scale ionospheric disturbances, we showed in the map (Fig. 1b, filled circles) the positions of the sub-ionospheric points, corresponding to the maximums in the TEC variations filtered within the range of periods 32–128 min at 0900–1100 UT on August 7, 2006 (1800–2000 LT for  $135^{\circ}\text{E}$ ). Approximately within the same time interval, the maximum intensity in  $S_L(t)$  was observed (Fig. 3a). It is evident that the registered maximums of large-scale disturbances are located near the region of maximum typhoon activity (a circle in Fig. 1b). On the other hand, almost all maximums are located on the dusk side of the equatorial anomaly northern ridge (the map of absolute TEC values is shown by the gradations of gray color in Fig. 1b).

As far as an increase in the  $S_L(t)$  intensity is observed during the storm maximum phase, we can assume that this phenomenon was related to enhanced activity of large-scale TIDs (which could reach the region of typhoon action, propagating from the region of their generation in the auroral zone) and to the complicated dynamics of the equatorial anomaly disturbed under the magnetic storm conditions.

The maximum values of the TEC intensity variations  $S_M(t)$  (10–25 min) and  $S_S(t)$  (2–10 min) in two other ranges of periods were observed on August 3, 2006, and August 4, 2006, before the typhoon appear-

ance (Figs. 3b, 3c). During the time of the typhoon existence, no intensification of the  $S_M(t)$  and  $S_S(t)$  variations as compared to the adjacent days was observed.

#### 4. DISCUSSION AND CONCLUSIONS

In the region of typhoon action during the magnetic storm on August 7, 2006, an increase in TEC variations in the evening local time was detected within the range of periods 32–128 min. In spite of the fact that the corresponding extremums in the TEC variations were registered near the region of typhoon action, it is difficult to conclude that these events were interrelated. Most probably this effect was caused by the dynamics of the disturbed irregular structure of the equatorial anomaly and by the appearance of intense large-scale auroral disturbances at low latitudes. An analysis of the diurnal variations in the TEC absolute values and TEC variations with periods of 2–25 min indicated that the TEC intensity did not substantially increase during the period of typhoon action as compared to the adjacent days.

Thus, an analysis of the intensity of TEC variations, determined using the data of ground-based GPS receivers and GIM maps, revealed no ionospheric disturbances unambiguously related to the SAOMAI-2006 typhoon.

#### ACKNOWLEDGMENTS

We thank the staff of Scripps Orbit and Permanent Array Center (SOPAC) for presented initial data from the global network of ground-based two-frequency GPS receivers.

The work was supported by the Russian Foundation for Basic Research (project nos. 06-05-64577 and 06-05-64577) and by the Siberian Branch of the Russian Academy of Sciences (integration project No. 3.24).

#### REFERENCES

1. E. L. Afraimovich, "GPS Global Detection of the Ionospheric Response to Solar Flares," *Radio Sci.* **35**, 1417–1424 (2000).
2. F. Bertin, J. Testud, and L. Kersley, "Medium Scale Gravity Waves in the Ionospheric  $F$ -Region and Their Possible Origin in Weather Disturbances," *Planet. Space Sci.* **23**, 493–507 (1975).
3. M. J. Buonsanto, "Ionospheric Storms - A Review," *Space Sci. Rev.* **88**, 563–601 (1999).
4. D. H. Cowling, H. D. Webb, and K. C. Yeh, "Group Rays of Internal Gravity Waves in a Stratified Atmosphere," *J. Geophys. Res.* **76**, 213–220 (1971).
5. K. Davies and J. E. Jones, "Acoustic Waves in the Ionospheric  $F_2$ -Region Produced by Severe Thunderstorms," *J. Atmos. Terr. Phys.* **35**, 1737–1744 (1973).
6. K. Davies and J. E. Jones, "Ionospheric Disturbances in the  $F_2$ -Region Associated with Severe Thunderstorms," *J. Atmos. Sci.* **28**, 254–262 (1971).
7. J. M. Forbes, S. E. Palo, and X. Zhang, "Variability of the Ionosphere," *J. Atmos. Sol.-Terr. Phys.* **62**, 685–693 (2000).
8. K. Hocke and K. Schegel, "A Review of Atmospheric Gravity Waves and Traveling Ionospheric Disturbances: 1982–1995," *Ann. Geophys.* **14**, 917–940 (1996).
9. B. Hofmann-Wellenhof, H. Lichtenegger, and J. Collins, *Global Positioning System: Theory and Practice* (Springer, New York, 1992).
10. Y.-N. Huang, K. Cheng, and S.-W. Chen, "On the Detection of Acoustic-Gravity Waves Generated by Typhoon by Use of Real Time HF Doppler Frequency Shift Sounding System," *Radio Sci.* **20**, 897–906 (1985).
11. E. S. Kazimirovsky and V. D. Kokourov, *Motion in the Ionosphere* (Nauka, Novosibirsk, 1979) [in Russian].
12. J. A. Klobuchar, "Ionospheric Time-Delay Algorithm for Single-Frequency GPS Users," *IEEE Trans. Aerospace Electron. Syst.* **23** (3), 325–331 (1986).
13. A. J. Mannucci, B. D. Wilson, D. N. Yuan, et al., "A Global Mapping Technique for GPS-Derived Ionospheric TEC Measurements," *Radio Sci.* **33** (3), 565–582 (1998).
14. D. Pancheva, N. Mitchell, R. R. Clark, et al., "Variability in the Maximum Height of the Ionospheric  $F_2$ -Layer over Millstone Hill (September 1998–March 2000): Influence from below and above," *Ann. Geophys.* **20**, 1807–1819 (2002).
15. S. S. Prasad, L. J. Schneck, and K. Davies, "Ionospheric Disturbances by Severe Tropospheric Weather Storms," *J. Atmos. Terr. Phys.* **37**, 1357–1363 (1975).
16. V. M. Sorokin, V. M. Chmyrev, and A. K. Yaschenko, "Electrodynamic Model of the Lower Atmosphere and the Ionosphere Coupling," *J. Atmos. Terr. Phys.* **63**, 1681–1691 (2001).
17. J. A. Waldock and T. B. Jones, "The Effects of Neutral Winds on the Propagation of Medium-Scale Atmospheric Gravity Waves at Mid-Latitudes," *J. Atmos. Terr. Phys.* **46**, 217–231 (1984).